Original Article

Comparison of pulmonary artery sarcoma and pulmonary thromboembolism according to clinical and computed tomography pulmonary angiography and magnetic resonance imaging characteristics: a single-center retrospective study

Runcai Guo[1], Haoyu Yang[2], Linfeng Xi[3], Anqi Liu[4], Mei Deng[4], Hongyan Liu[5], Qian Gao[3], Wanmu Xie[3], Yanan Zhen[6], Zhenguo Huang[1], Min Liu[1]

[1]Department of Radiology, China-Japan Friendship Hospital, Beijing, China; [2]Department of Radiology, Peking University China-Japan Friendship School of Clinical Medicine, Beijing, China; [3]Department of Pulmonary and Critical Care Medicine, Center of Respiratory Medicine, China-Japan Friendship Hospital National Center for Respiratory Medicine, Beijing, China; [4]Department of Radiology, China-Japan Friendship Hospital of Chinese Academy of Medical Sciences and Peking Union Medical College, Beijing, China; [5]Department of Pathology, China-Japan Friendship Hospital, Beijing, China; [6]Department of Cardiovascular Surgery, China-Japan Friendship Hospital, Beijing, China

Contributions: (I) Conception and design: M Liu; (II) Administrative support: M Liu, Z Huang; (III) Provision of study materials or patients: L Xi, A Liu, M Deng, H Liu, Q Gao, W Xie, Y Zhen; (IV) Collection and assembly of data: R Guo, H Yang, L Xi, A Liu, M Deng, H Liu, Q Gao; (V) Data analysis and interpretation: R Guo, H Yang, L Xi, A Liu; (VI) Manuscript writing: All authors; (VII) Final approval of manuscript: All authors.

Correspondence to: Min Liu, MD. Department of Radiology, China-Japan Friendship Hospital, No. 2 Yinghua Dong Street, Hepingli, Chaoyang District, Beijing 100029, China. Email: mikie0763@126.com.

Background: Pulmonary artery sarcoma (PAS) is a very rare malignancy with a poor prognosis; however, its clinical manifestations and imaging findings are often indistinguishable from pulmonary thromboembolism (PTE). We thus aimed to accurately diagnose PAS by comparing the clinical and computed tomography pulmonary angiography (CTPA) and magnetic resonance imaging (MRI) imaging characteristics of PAS and PTE.

Methods: This case-control study retrospectively enrolled 20 patients with PAS (from March 2017 to September 2022), 40 patients with central acute PTE, and 40 patients with central chronic PTE (from January 2021 to December 2022) in the China-Japan Friendship Hospital. The following clinical and imaging findings were compared between the three groups: initial symptoms; D-dimer, C-reactive protein, and N-terminal pro B-type natriuretic peptide levels; wall-eclipsing sign (WES); scope of lesion involvement; and morphological characteristics. Signal intensity was also observed on different MRI sequences.

Results: The D-dimer level in PAS was significantly lower than that in central acute PTE (P<0.001). The WES was present in 17 cases of PAS (85.0%), which was a greater proportion than that of the central acute PTE and chronic PTE groups (all P values <0.001). The involvement of the pulmonary valve or right ventricular outflow tract was observed in five PAS cases but none of the central acute PTE or chronic PTE cases (all P values =0.001). In 19 PAS cases (95.0%), the lesions grew expansively in the central pulmonary artery. The proximal margin of 18 patients with PAS (90.0%) was bulging or lobulated. Nine cases of PAS (45.0%) showed aneurysm-like dilatation (grape-like sign) of the distal pulmonary artery, representing significantly greater proportion than that of the central acute PTE and chronic PTE groups (all P values <0.001). In 37 patients with central acute PTE (92.5%), the clots were observed to be floating in the pulmonary artery lumen with saddle, tubular or polypoid shape. Eccentric filling defects attached to the pulmonary artery wall were observed in 32 cases of central chronic PTE (80.0%). On MRI, PAS lesions were hyperintense on fat-suppressed T2-weighted imaging and diffusion-weighted imaging, demonstrating heterogeneous enhancement.

Conclusions: Comprehensive analysis of the clinical data and imaging features on CTPA and MRI can aid in the accurate differential diagnosis of PAS and PTE.

Keywords: Pulmonary artery sarcoma (PAS); pulmonary thromboembolism (PTE); computed tomography pulmonary angiography (CTPA); magnetic resonance imaging (MRI)

Submitted Jul 11, 2023. Accepted for publication Dec 05, 2023. Published online Jan 23, 2024.
doi: 10.21037/qims-23-992
View this article at: https://dx.doi.org/10.21037/qims-23-992

Introduction

Pulmonary artery sarcoma (PAS), which primarily originates from the pulmonary artery, is an extremely rare malignancy (1). PAS was first reported in 1923 (2), and due to the low incidence of PAS, most related studies have been case reports, with only a few small-sample studies reported in the literature. The etiology and risk factors of PAS are still unclear, and it is usually incurable and involves a very poor prognosis; therefore, early diagnosis and radical surgery provide the only survival chance for patients with this disease (3).

Since PAS consistently presents with filling defects in the pulmonary artery on computed tomography pulmonary angiography (CTPA) and magnetic resonance imaging (MRI), it is highly similar to pulmonary thromboembolism (PTE) (4,5). Moreover, PAS often involves the main pulmonary artery and left and right pulmonary arteries and occasionally the pulmonary valve and right ventricular outflow tract (6). A few studies have reported upon the differences in imaging characteristic between PAS and chronic pulmonary thromboembolism (CPTE) (4,7). However, the clinical manifestation and imaging features of patients with PAS are very similar to those with acute pulmonary thromboembolism (APTE). In cases where patients with suspected APTE fail to respond to anticoagulant therapy, PAS is considered as a differential diagnosis, and thus it frequently leads to misdiagnosis and mistreatment.

In order to facilitate the timely differential diagnosis of PTE, with which PAS is most commonly confused, we conducted a retrospective analysis of the clinical manifestations and CTPA and MRI findings of PAS, central APTE, and CPTE in this study. We present this article in accordance with the STROBE reporting checklist (available at https://qims.amegroups.com/article/view/10.21037/qims-23-992/rc).

Methods

Study population

This case-control study was conducted in accordance with the Declaration of Helsinki (as revised in 2013) and was approved by the institutional review board of the China-Japan Friendship Hospital (No. 2023-KY-070). Informed consent was waived due to the retrospective nature of this study. A total of 20 patients diagnosed with PAS from March 2017 to September 2022 were included in this study, comprising 11 cases of pulmonary artery intimal sarcoma, 3 cases of pleomorphic fascicular sarcoma, 2 cases of osteosarcomatous sarcoma, 1 case of leiomyosarcoma, and 3 cases of unclassifiable sarcomas, in the China-Japan Friendship Hospital. Additionally, 40 patients diagnosed with APTE and 40 patients diagnosed with CPTE at the China-Japan Friendship Hospital between January 2021 and December 2022 were included as comparison groups. The ratio of patients with PAS to those with APTE and those with CPTE was 1:2:2. Central PTE was defined as embolus involving the main pulmonary artery or left or right pulmonary artery trunk. All included patients underwent CTPA in China-Japan Friendship Hospital, among whom 12 patients with PAS and 5 patients with CPTE underwent MRI, and 12 patients with PAS and 2 patients with CPTE underwent F-18-fluorodeoxyglucose positron emission tomography/computed tomography (^{18}F-FDG PET/CT). APTE was diagnosed if pulmonary artery filling defects on CTPA were significantly reduced or absorbed after sufficient anticoagulant therapy was administered for 1 month. After pulmonary artery endarterectomy or biopsy was performed, pathological diagnoses of CPTE and PAS were confirmed. The baseline clinical information of patients, including initial symptoms and D-dimer, C-reactive protein (CRP), and N-terminal pro B-type natriuretic peptide (NT-proBNP) levels, was collected from the medical charts. The exclusion criteria were as follows:

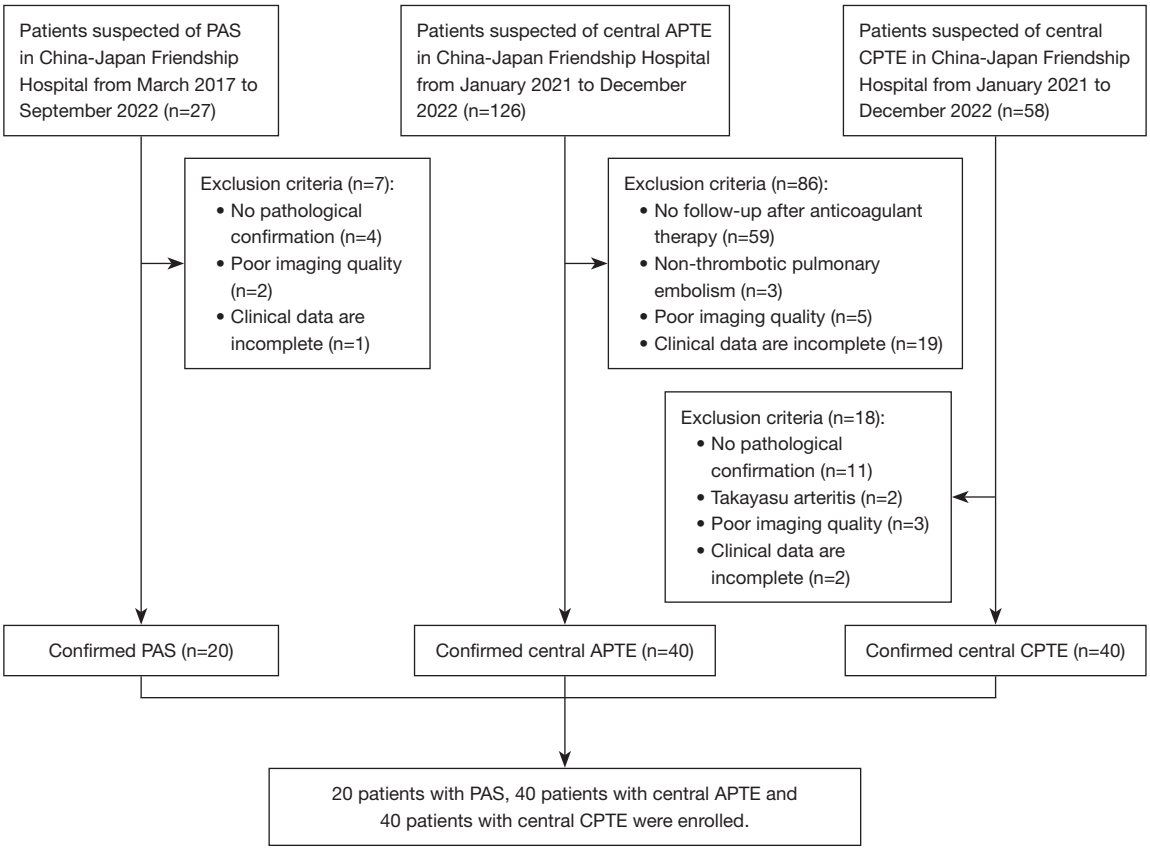

Figure 1 Flowchart of patient selection. PAS, pulmonary artery sarcoma; APTE, acute pulmonary thromboembolism; CPTE, chronic pulmonary thromboembolism.

(I) no pathological confirmation of PAS and CPTE, (II) no follow-up on patients with APTE after anticoagulant therapy, (III) nonthrombotic pulmonary embolism, (IV) Takayasu arteritis, (V) poor imaging quality, and (VI) incomplete clinical data. The enrollment of patients is shown in *Figure 1*.

CT scan protocols

All patients underwent supine CTPA with either a 256-row CT (GE Revolution CT, GE HealthCare, Waukesha, WI, USA) or a 320-row CT (Aquilion ONE, Canon Medical Systems, Otawara, Tochigi, Japan) at the end of expiration, with the lung being covered from the base to the apex. The parameters for CTPA scanning were as follows: 120 kV, 100–300 mAs, 0.8 second rotation time, 0.625 to 1-mm slice thickness, and 0.625 to 1-mm slice interval. Patients were injected with a bolus of 70 mL nonionic contrast (370 mgI/mL; Ultravist, Bayer, Guangzhou, China) at a rate of 4–4.5 mL/s, which was followed by a 50-mL saline injection at the same rate. Bolus-tracking technology was used to obtain good contrast enhancement images with the trigger threshold of 100 HU on the main pulmonary artery. The field of view (FOV) covered an area of 300×300 mm^2, and the matrix was 512×512.

MRI scan protocols

MRI was performed using a 1.5T MRI scanner (MAGNETOM Aera, Siemens Healthineers, Erlangen, Germany). The scan protocol consisted of the following sequences: T1-weighted imaging [T1WI; repetition time (TR) 639 ms, echo time (TE) 27 ms, FOV 340×340 mm^2, matrix 256×256, slice thickness 6 mm], fat-suppressed T2-weighted imaging (T2WI; TR 3,260 ms, TE 86 ms, FOV 400×400 mm^2, matrix 256×256, slice thickness 6 mm), and diffusion-weighted imaging (DWI; b 0 and 1,000 s/mm^2, TR 6,300 ms, TE 49 ms, FOV 380×380 mm^2, matrix

128×128, slice thickness 5 mm). After the noncontrast sequences, a dynamic contrast-enhanced sequence was obtained with a three-dimensional volumetric interpolated breath-hold sequence (3D-VIBE; TR 6.67 ms, TE 2.39 ms, FOV 400×400 mm^2, matrix 320×320, slice thickness 3 mm). Patients were injected with gadopentetate dimeglumine (0.2 mmol/kg; Magnevist, Bayer) at a rate of 3 mL/s, which was followed by a 30-mL saline injection at the same rate.

Imaging analysis

All CTPA and MRI images were analyzed on a picture archiving and communication system workstation by two chest radiologists with 10- and 16-year-experience who were blinded to the patient's clinical diagnosis. Decisions were made via discussion by the two radiologists.

The imaging features on CTPA include the following: (I) the location of the filling defect, (II) the involvement of the pulmonary valve or right ventricular outflow tract, and (III) the morphological characteristics of the filling defect. The morphology of filling defect was mainly divided into three types: (I) complete filling defect/expansive growth; (II) eccentric filling defect attached to the pulmonary artery wall; and (III) saddle, tubular, or polypoid filling defect in the pulmonary artery lumen (8). The following parameters were recorded: (I) wall-eclipsing sign (WES) (9), (II) proximal bulging or lobular shape or proximal flat shape, (III) distal aneurysm-like dilatation (grape-like sign) or stenosis, (IV) calcification within the lesion, (V) collateral circulation in the mediastinum, (VI) pleural effusion, and (VII) pericardial effusion. WES was defined as a lesion that invades the pulmonary artery wall while occupying almost the entire lumen of the pulmonary artery, with the proximal margin of the lesion protruding into the right ventricular outflow tract (9). Distal dilatation was defined as a pulmonary artery diameter of at least 1.5 times the normal pulmonary artery diameter at the same level of the contralateral lung. Moreover, the following parameters were measured: right ventricular transversal diameter (RVd), left ventricular transversal diameter (LVd), diameter of main pulmonary artery (MPAd), and diameter of ascending aorta (AAd).

Only a small number of patients with PAS and CPTE underwent MRI. This study conducted a preliminary analysis of the signal characteristics on noncontrast and contrast sequences. Through a comparison of the signal intensity of the chest wall, the intensity of the filling defect in the pulmonary artery was categorized as hyperintense, moderately hyperintense, isointense, moderately hypointense, and hypointense on noncontrast MRI (5). The enhancement of the filling defect was also evaluated.

Statistical analysis

Continuous variables are expressed as mean ± standard deviation (SD) and were compared with the *t*-test. If data did not conform to a normal distribution, they were compared with the Mann-Whitney test and are expressed as median with interquartile range (IQR). Categorical data are expressed as a percentage and were compared with the χ^2 test or Fisher exact test. Statistical analyses were performed using SPSS 17.0 (IBM Corp.). A two-sided P value <0.05 was considered to be statistically significant.

Results

Clinical manifestations

Table 1 displays the clinical features in patients with PAS, central APTE, and CPTE. Patients with PAS (7 males, mean age 47.1±13.2 years) were significantly younger than those with APTE (P<0.001) and had a similar age as did those with CPTE (P=0.198). The gender distribution was comparable between the three groups. The incidence of deep vein thrombosis (DVT) was found to be significantly higher in patients with central APTE compared to those with PAS (P=0.001), but there was no significant difference between PAS and central CPTE. Although dyspnea, chest pain, cough, and hemoptysis among the three groups were different, they were the common symptoms in the three groups. Furthermore, patients with PAS, compared to patients with APTE, had considerably lower D-dimer (P<0.001), CRP (P=0.007), and NT-proBNP (P<0.001) levels. The CRP level of patients with PAS was significantly higher than that of patients with CPTE (P=0.026), whereas the NT-proBNP level was significantly higher in patients with CPTE (P=0.001).

Imaging features on CTPA

Table 2 shows the CTPA imaging findings among patients with PAS, central APTE, and CPTE. The frequency of main pulmonary artery involvement in the PAS group (*Figure 2*) was significantly higher than that in the central APTE and CPTE groups (all P values <0.001). PAS and central APTE tended to involve the bilateral central pulmonary arteries (*Figures 2,3*), while central CPTE was

Table 1 Clinical manifestations in patients with pulmonary artery sarcoma and central pulmonary thromboembolism

Variable	PAS (n=20)	Central APTE (n=40)	Central CPTE (n=40)	P value†	P value‡
Age (years), mean ± SD	47.1±13.2	64.9±14.4	51.7±12.9	<0.001*	0.198
Men, n (%)	7 (35.0)	19 (47.5)	23 (57.5)	0.357	0.100
Dyspnea, n (%)	6 (30.0)	24 (60.0)	9 (22.5)	0.028*	0.527
Chest pain, n (%)	12 (60.0)	6 (15.0)	5 (12.5)	<0.001*	<0.001*
Cough/sputum, n (%)	12 (60.0)	4 (10.0)	10 (25.0)	<0.001*	0.008*
Hemoptysis, n (%)	7 (35.0)	2 (5.0)	9 (22.5)	0.007*	0.302
Fever, n (%)	3 (15.0)	7 (17.5)	3 (7.5)	>0.99	0.648
Syncope, n (%)	2 (10.0)	4 (10.0)	5 (12.5)	>0.99	>0.99
Shortness of breath, n (%)	8 (40.0)	7 (17.5)	23 (57.5)	0.058	0.201
Weight loss, n (%)	3 (15.0)	2 (5.0)	4 (10.0)	0.409	0.887
DVT of the lower limbs, n (%)	4 (20.0)	27 (67.5)	14 (35.0)	0.001*	0.370
D-dimer (mg/L), median [IQR]	0.5 [0.4–0.8]	23.0 [10.2–52.7]	0.6 [0.4–1.3]	<0.001*	0.525
CRP (mg/L), median [IQR]	9.1 [3.6–30.3]	14.0 [3.3–81.9]	2.8 [2.5–11.2]	0.007*	0.026*
NT-proBNP (pg/mL), median [IQR]	72.0 [31.5–166.5]	888.5 [249.8–3,111.3]	765.0 [140.3–2,122.0]	<0.001*	0.001*
Response to anticoagulant therapy	No	Yes	No	–	–
Pulmonary endarterectomy	12	0	40	–	–
Biopsy	8	0	0	–	–

†, comparison between PAS and APTE; ‡, comparison between PAS and CPTE; *, P<0.05. PAS, pulmonary artery sarcoma; APTE, acute pulmonary thromboembolism; CPTE, chronic pulmonary thromboembolism; SD, standard deviation; DVT, deep vein thrombosis; IQR, interquartile range; CRP, C-reactive protein; NT-proBNP, N-terminal pro B-type natriuretic peptide.

more commonly found in the unilateral central pulmonary artery (*Figure 4*). In five cases of PAS, the lesions involved the pulmonary valve or right ventricular outflow tract, which was not observed in any of the patients with APTE or CPTE (all P values =0.001). In 19 patients with PAS (95.0%), the lesions grew expansively in the main and/or bilateral central pulmonary arteries (*Figures 2,5*). WES was present in 17 patients with PAS (85.0%) (*Figure 2*) but not in any of the patients with central APTE or CPTE (all P values <0.001). The proximal margin of 18 patients with PAS (90.0%) was bulging or lobulated (*Figures 2,5*), and the distal pulmonary artery of 9 patients with PAS (45.0%) showed aneurysm-like dilatation, a feature we refer to as "grape-like" sign (*Figure 2*).

In 37 patients with APTE (92.5%), a new thrombus was observed to be floating in the pulmonary artery lumen with a saddle, tubular, or polypoid shape (*Figure 3*) and proximal bulging shape but no stenosis or dilatation of the distal pulmonary artery.

One month after anticoagulant therapy, the new thrombus in the central pulmonary arteries was significantly reduced on CTPA (*Figure 3*). The clots in 32 patients with CPTE (80.0%) manifested eccentric filling defects which formed an obtuse angle with the pulmonary artery wall (*Figure 6*), while the filling defects in the patients with PAS or central APTE formed an acute angle. The proximal margin of the CPTE lesions was flat in 22 cases (55.0%), and the distal pulmonary artery lumen showed stenosis or occlusion in 14 cases (35.0%).

Lung and pleura metastases were observed in four patients with PAS (*Figure 2*), and one patient showed multiple systemic metastases. Calcification was observed in eight patients with CPTE (*Figure 6*) and four patients with PAS, but not in any patients with APTE. Collateral circulation was found in 26 patients with CPTE (*Figure 6*), five with PAS, and one with APTE. The ratios of RVd to LVd and MPAd to AAd in the CPTE group were significantly higher than those of the PAS group (all P values =0.001). Moreover, there was a heterogenous increase in ^{18}F-FDG uptake in all 12 patients with PAS in

Table 2 Comparison of imaging findings in patients with pulmonary artery sarcoma and central pulmonary thromboembolism

Imaging findings	PAS (n=20)	Central APTE (n=40)	Central CPTE (n=40)	P value†	P value‡
Wall-eclipsing sign, n (%)	17 (85.0)	0	0	<0.001*	<0.001*
Main pulmonary artery involvement, n (%)	19 (95.0)	6 (15.0)	5 (12.5)	<0.001*	<0.001*
Right and left pulmonary artery involvement, n (%)	15 (75.0)	26 (65.0)	10 (25.0)	0.432	<0.001*
Pulmonary valve or right ventricular outflow tract involvement, n (%)	5 (25.0)	0	0	0.001*	0.001*
Complete filling defect/expansive growth, n (%)	19 (95.0)	1 (2.5)	7 (17.5)	<0.001*	<0.001*
Eccentric filling defect attached to the pulmonary artery wall, n (%)	1 (5.0)	2 (5.0)	32 (80.0)	>0.99	<0.001*
Saddle, tubular, or polypoid filling defect in the pulmonary artery lumen, n (%)	0	37 (92.5)	1 (2.5)	<0.001*	0.480
Proximal bulging or lobular shape, n (%)	18 (90.0)	35 (87.5)	7 (17.5)	0.776	<0.001*
Proximal flat shape, n (%)	1 (5.0)	5 (12.5)	22 (55.0)	0.648	0.001*
Distal aneurysm-like dilatation (grape-like sign), n (%)	9 (45.0)	0	0	<0.001*	<0.001*
Distal stenosis, n (%)	1 (5.0)	0	14 (35.0)	0.157	0.027*
Calcification within the lesion, n (%)	4 (20.0)	0	8 (20.0)	0.004*	>0.99
Collateral circulation in the mediastinum, n (%)	5 (25.0)	1 (2.5)	26 (65.0)	0.022*	0.003*
Pleural effusion, n (%)	9 (45.0)	7 (17.5)	8 (20.0)	0.023*	0.043*
Pericardial effusion, n (%)	1 (5.0)	5 (12.5)	9 (22.5)	0.648	0.178
RVd:LVd ratio, mean ± SD	0.9±0.1	1.0±0.1	1.1±0.2	0.001*	0.001*
MPAd:AAd ratio, mean ± SD	0.9±0.1	0.9±0.2	1.2±0.2	0.976	0.001*

†, comparison between PAS and APTE; ‡, comparison between PAS and CPTE; *, P<0.05. PAS, pulmonary artery sarcoma; APTE, acute pulmonary thromboembolism; CPTE, chronic pulmonary thromboembolism; RVd, right ventricular transversal diameter; LVd, left ventricular transversal diameter; MPAd, diameter of main pulmonary artery; AAd, diameter of ascending aorta; SD, standard deviation.

terms of maximum standardized uptake value (SUVmax), with a median value of 9.1 (IQR, 3.9–16.8) on PET/CT (Figure S1), while two patients with CPTE had low ^{18}F-FDG uptake (SUVmax =1.2 and 1.0).

Signal intensity on MRI

No patients with APTE underwent MRI before anticoagulant therapy. *Table 3* shows the signal intensity of PAS and central CPTE lesions on different sequences of MRI. On fat-suppressed T2WI, 12 PAS lesions (100%) were moderately hyperintense (*Figure 5*) or hyperintense, while four CPTE lesions were hypointense (*Figure 4*) or isointense (χ^2=11.815; P=0.001). On T1WI, eight PAS lesions were isointense (*Figure 5*), and four were moderately hyperintense, which was similar to the findings for CPTE (χ^2=0.975; P=0.323). Ten PAS lesions (83.3%) were moderately hyperintense or hyperintense on DWI, and nine were hypointense on apparent diffusion coefficient (ADC) (*Figure 5*), indicating diffusion restriction, but none of CPTE lesions showed diffusion restrictions (*Figure 4*) (χ^2=5.834; P=0.016). All PAS lesions (100%) were heterogeneously enhanced (*Figure 5*), while four CPTE (80.0%) lesions were not obviously enhanced on the contrast 3D-VIBE sequence (*Figure 4*) (χ^2=11.815; P=0.001).

Discussion

In order to facilitate the timely and accurately diagnosis of PAS, we compared the clinical and imaging findings of patients with PAS, central APTE, and CPTE. The principal findings were the following: (I) the serum D-dimer level of PAS was significantly lower than that of APTE, and the CRP level of PAS was significantly higher than that of CPTE but lower than that of APTE. (II) WES and invasion of the pulmonary valve or right ventricular

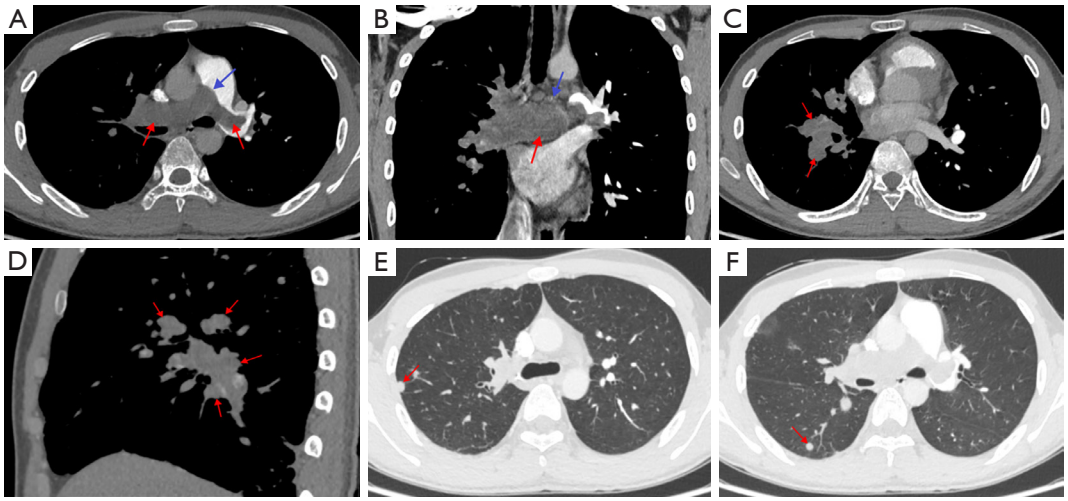

Figure 2 A 19-year-old man with a pathological diagnosis of pulmonary artery sarcoma. (A) CTPA axial image showed filling detects located in the main and bilateral pulmonary arteries (red arrows), with a bulging proximal margin of the lesion (blue arrow). (B) CTPA coronal imaging showed that a mass had grown expansively in the right pulmonary artery (red arrow), occupying the entire lumen and eclipsing the pulmonary artery wall (wall-eclipsing sign) (blue arrow). (C,D) CTPA axial and sagittal images showed that the lesion was filling the right middle and lower lobe pulmonary arteries along its course giving it a grape-like sign (red arrows). (E,F) Multiple metastatic tumors in the right lung (red arrows). CTPA, computed tomography pulmonary angiography.

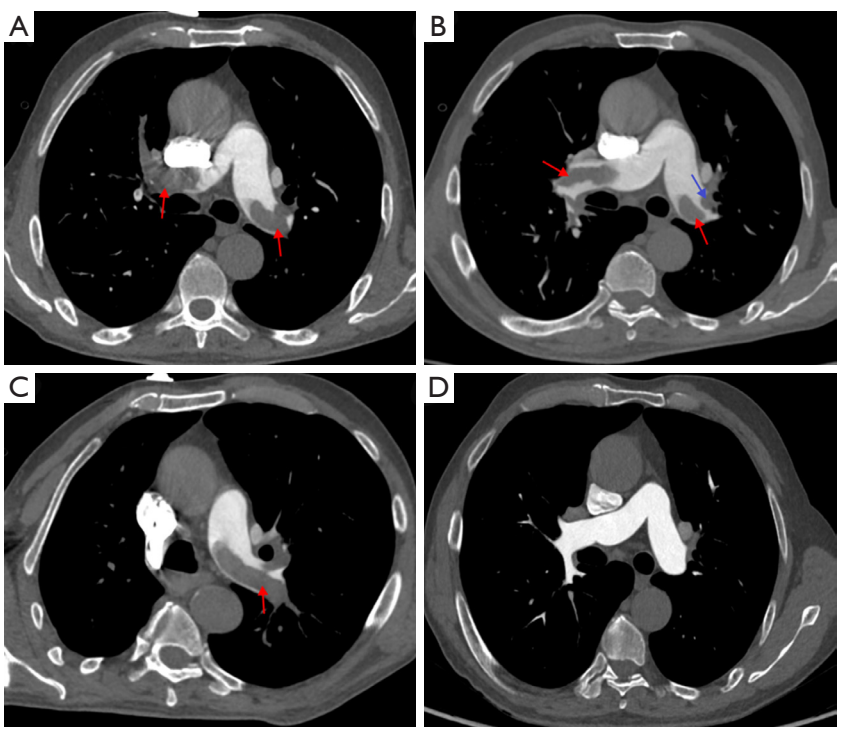

Figure 3 A 67-year-old man with sudden syncope and deep vein thrombosis of the lower limbs was clinically diagnosed with acute pulmonary thromboembolism. (A) CTPA axial imaging showed filling detects in the bilateral pulmonary arteries (red arrows). (B,C) CTPA oblique axial images showed emboli floating in the lumen of the pulmonary artery with a tubular (red arrows) or polypoid (blue arrow) shape. (D) One month after anticoagulant therapy, CTPA axial imaging showed that the filling detects in the bilateral pulmonary arteries had significantly reduced. CTPA, computed tomography pulmonary angiography.

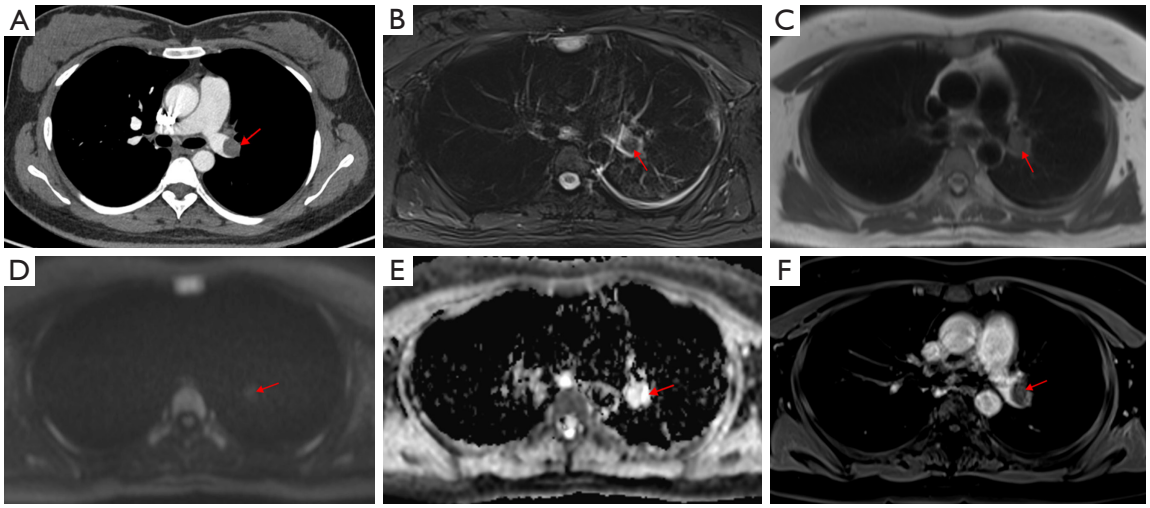

Figure 4 A 35-year-old man with a pathological diagnosis of chronic pulmonary thromboembolism. (A) Computed tomography pulmonary angiography showed a nodular filling defect in the left pulmonary artery (red arrow). (B) The lesion was hypointense on fat-suppressed T2-weighted imaging (red arrow). (C) T1-weighted imaging showed an isointense nodular lesion in the left pulmonary artery (red arrow). (D) On diffusion-weighted imaging (b =1,000 s/mm2), the lesion was isointense (red arrow). (E) The lesion was hyperintense on apparent diffusion coefficient map (red arrow), indicating no diffusion restriction. (F) On enhancement imaging, the lesion was not obviously enhanced (red arrow).

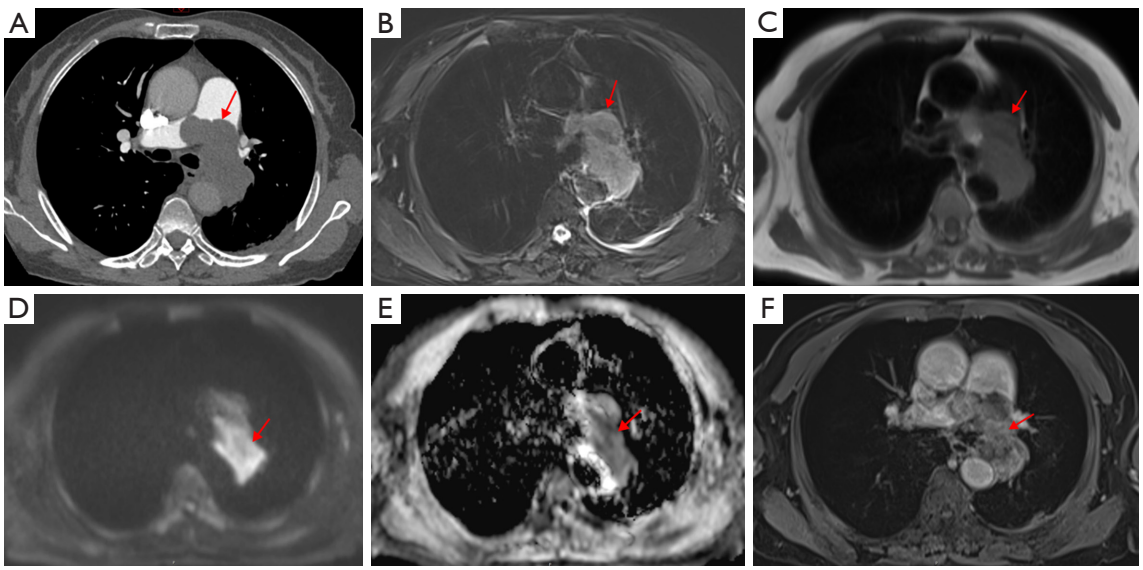

Figure 5 A 57-year-old woman with pathological diagnosis of pulmonary artery sarcoma. (A) Computed tomography pulmonary angiography, showed filling detects located in the main and bilateral pulmonary arteries, and the proximal margin of the lesion was bulging and lobular (red arrow). (B) Fat-suppressed T2-weighted imaging showed a moderately hyperintense mass in the main and bilateral pulmonary arteries, and the proximal margin was bulging (red arrow). (C) T1-weighted imaging showed an isointense mass in the pulmonary artery (red arrow). Hyperintensity on diffusion-weighted imaging (red arrow) (D) corresponded with hypointensity on the apparent diffusion coefficient map (red arrow) (E), indicating diffusion restriction. (F) The lesion was heterogeneously enhanced (red arrow).

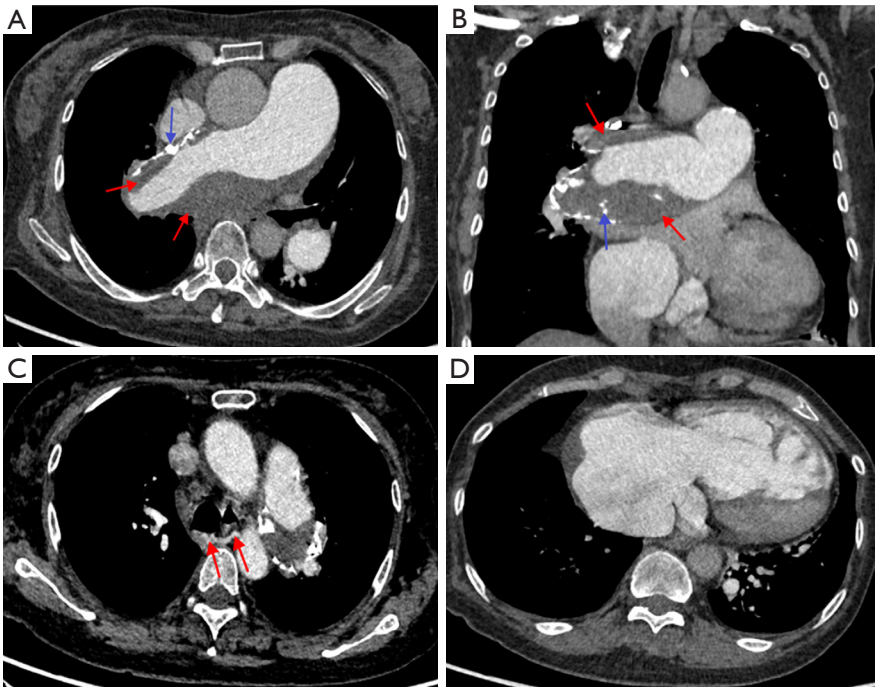

Figure 6 A 59-year-old woman with a pathological diagnosis of chronic pulmonary thromboembolism. (A,B) CTPA axial and coronal images showed eccentric filling detects attached to the right pulmonary artery wall (red arrows), calcification within the lesion and on the pulmonary artery wall (blue arrows), and dilatation of the main pulmonary artery. (C) CTPA axial imaging showed collateral circulation in the mediastinum (red arrows). (D) A significantly dilated right atrium and ventricle suggested right heart dysfunction. CTPA, computed tomography pulmonary angiography.

outflow tract were imaging features of PAS, and PAS lesions were characterized by proximal bulging or lobular shape and a grape-like sign in the distal pulmonary artery. (III) PAS showed hyperintensity on fat-suppressed T2WI and DWI and heterogeneous enhancement. (IV) The eccentric filling defects attached to pulmonary artery wall showing hypointensity on fat-suppressed T2WI and no enhancement was characteristic of CPTE.

Sarcoma of the great vessels is a rare malignant tumor with an incidence only ranging between 0.001% and 0.030% (10), whereas the true incidence of PAS remains unknown since it is an extremely rare but devastating disease. In one study, the average age of individuals diagnosed with PAS was 48 years, and the ratio of females to males was 1.3:1 (11). Similarly, in our study, the average age of patients with PAS was 47.1±13.2 years, with 13 females and 7 males. It thus seems that PAS is more common in middle-aged women. The nonspecific clinical symptoms of patients with PAS mainly include dyspnea, chest pain, cough, hemoptysis, shortness of breath, fever, and syncope (12), which are also common in patients with PTE. One study proposed the characteristic clinical manifestations of PAS to be fever, fatigue, and malignant tumor-related weight loss (13). A higher frequency of DVT and a significantly increased D-dimer level are valuable indicators of APTE. In another study, the NT-proBNP level in patients with PAS was lower than that of those with APTE and CPTE, while BNP in patients with PAS was lower than that of those with PTE (8). This may indicate that the right heart dysfunction in PTE is more severe than that in PAS.

Both PAS and central APTE tended to involve bilateral pulmonary arteries, while central CPTE was more common in the unilateral pulmonary artery. Importantly, only PAS involved the pulmonary valve and right ventricular outflow tract, and this was not observed in either patients with central APTE or CPTE. Cox *et al.* (14) reported that 85%, 71%, 65%, 32%, and 10% of patients with PAS involved the main pulmonary artery, right pulmonary artery, left pulmonary artery, pulmonary valve, and right ventricular outflow tract, respectively, which was similar to our findings. We speculate that the faster blood flow in the main pulmonary artery, pulmonary valve, and right

Table 3 Signal intensity characteristics of pulmonary artery sarcoma and central chronic pulmonary thromboembolism on MRI

Patient	Gender	Age (years)	T1WI	Fat-suppressed T2WI	Diffusion	Enhancement	Pathological diagnosis
1	Female	53	Isointense	Moderately hyperintense	Restricted	Yes	PAS
2	Female	42	Isointense	Moderately hyperintense	Normal	Yes	PAS
3	Male	21	Moderately hyperintense	Hyperintense	Restricted	Yes	PAS
4	Female	46	Isointense	Moderately hyperintense	Restricted	Yes	PAS
5	Female	66	Isointense	Moderately hyperintense	Restricted	Yes	PAS
6	Female	57	Isointense	Moderately hyperintense	Restricted	Yes	PAS
7	Female	62	Moderately hyperintense	Hyperintense	Normal	Yes	PAS
8	Male	54	Moderately hyperintense	Moderately hyperintense	Restricted	Yes	PAS
9	Female	58	Moderately hyperintense	Hyperintense	Normal	Yes	PAS
10	Male	41	Isointense	Moderately hyperintense	Restricted	Yes	PAS
11	Female	54	Isointense	Hyperintense	Restricted	Yes	PAS
12	Female	33	Isointense	Moderately hyperintense	Restricted	Yes	PAS
13	Female	55	Isointense	Isointense	Normal	No	CPTE
14	Male	57	Hyperintense	Hyperintense	Normal	Yes	CPTE
15	Female	61	Moderately hyperintense	Hypointense	Normal	No	CPTE
16	Male	20	Moderately hyperintense	Moderately hypointense	Normal	No	CPTE
17	Male	35	Isointense	Hypointense	Normal	No	CPTE

MRI, magnetic resonance imaging; T1WI, T1-weighted imaging; T2WI, T2-weighted imaging; PAS, pulmonary artery sarcoma; CPTE, chronic pulmonary thromboembolism.

ventricular outflow tract diminishes thrombus retention. Therefore, involvement of the main pulmonary artery, the pulmonary valve, and/or right ventricular outflow tract may be a characteristic indicator of PAS.

In this relatively large-sample study, we divided the morphology of the lesions into three main types. PAS showed expansive growth (95.0%), and only one lesion presented with the cauliflower-like filling defect attached to the pulmonary artery wall. Another study reported that 77.8% of PAS lesions grew expansively while the other lesions were attached to the pulmonary artery wall (4). Kim *et al.* reported that PAS showed expansive growth (61.5%), diffuse/focal wall thickening (23.1%), and cauliflower-like shape (15.4%) (8). Malignant tumors are progressive in growth, and different morphologies may correspond to different stages of tumor growth. We speculate that a cauliflower-like pattern may indicate an early stage of the tumor. The expansive growth of tumors is the dominant observation in the related literature. This may be because chest discomfort occurs only when the tumor grows expansively and even obstructs the pulmonary artery. In our study, a few central CPTE lesions showed expansive morphology (17.5%), which was related to the acute or subacute clot attached to organized embolism, while 80.0% of CPTE lesions presented with eccentric filling defects attached to the pulmonary artery wall. In 37 cases with central APTE (92.5%), the lesions were observed to be floating in the pulmonary artery lumen with saddle, tubular, or polypoid shape. PAS continues to grow into the proximal or distal pulmonary artery, so the lesion may show a bulging or lobulated shape at the proximal margin while the distal pulmonary artery is filled with tumor and expands outward, presenting a grape-like sign. In fact, one study reported this sign to be 100% specific to PAS (5). Therefore, the morphological characteristics of different lesions are helpful in distinguishing PAS from other conditions. Gan *et al.* (9) observed WES in all patients with PAS in their study, but none in the patients with APTE or CPTE. In our study, WES was present in 85.0% of the patients with PAS, so WES on CTPA was nearly pathognomonic for PAS.

Calcification was observed in both PAS and CPTE, which is in line with previous studies (15,16). Pathologically, calcification within the PAS lesion suggests that the tumor is accompanied by chondrosarcoma or osteosarcoma differentiation. Calcification of the thrombus is often found in patients with CPTE, along with the thickening and calcification of the pulmonary artery wall. Our study found that mediastinal collateral circulation was more common in the CPTE group than in the PAS and APTE group. More than half of the patients with CPTE developed collateral circulation in this study (15). This is because most patients with CTPE had pulmonary hypertension and right ventricular dysfunction (17). One hypothesis is that pulmonary artery obstruction in PAS has a more rapid progression compared with CPTE, so the right ventricle is less likely to generate such a high degree pulmonary hypertension (17). In another study, lung and mediastinal metastases were observed in about 50% of patients with PAS, and distant metastases occurred in 16–19% of these patients, and these were associated with poor survival (18).

In our study, both PAS and CPTE lesions on MRI T1WI were isointense or moderately hyperintense, which was thus not helpful for differentiating them. However, on fat-suppressed T2WI, all PAS lesions were hyperintense, while most of CPTE lesions were hypointense. DWI and ADC have been applied previously for the detection of tumor and further discrimination from nontumor (19). In our study, 10 patients with PAS (10/12) showed hyperintensity on DWI, nine of whom showed hypointensity on ADC, indicating diffusion restriction. However, none of the CPTE lesions showed diffusion restriction. A previous study (5) suggested that hyperintense filling defects on fat-suppressed T2WI with diffusion restriction on DWI may help to discriminate PAS from central CPTE. In our study, heterogeneous and/or delayed enhancement was the distinguishing feature of PAS on contrast MRI, as most CPTE lesions were not obviously enhanced. We speculated that the heterogeneous enhancement of PAS, may be attributable to the presence of necrosis, hemorrhage, calcification, and different pathological types. MRI is an evolving imaging modality for evaluating APTE in certain patient populations, such as pregnant patients or patients with contraindications to iodinated contrast (20,21). However, none of the patients in our study with suspected APTE underwent baseline MRI until they failed anticoagulant or thrombolytic therapy and PAS was suspected. Therefore, the signal intensity of APTE before anticoagulant or thrombolytic therapy remains unknown.

Our study found that the SUVmax of PAS was higher than PTE. Similar to the previous reports (22,23), PET/CT could distinguish PAS from PTE based on the SUVmax value, which is beneficial for the early diagnosis of PAS. However, patients with PAS demonstrated low FDG uptake, which could lead to a misdiagnosis of PTE (24). These features should be kept in mind in clinical practice.

Limitations

Some limitations to this study should be mentioned. First, we employed a single-center retrospective design, and not all patients, especially those with APTE, underwent MRI. Thus, the distinguishing features of APTE on MRI remain unknown. Second, short-term dynamic observation provides crucial information for the differential diagnosis of PTE and PAS. Unfortunately, our center currently does not have access to dynamic imaging for PAS. Third, further analysis is necessary to determine the relationship between the pathological types and imaging features of PAS. Finally, as PAS is very rare, we included all pathologically confirmed patients with PAS in China-Japan Friendship Hospital from 2017 to 2022 and compared them with patients with PTE. Therefore, no other PAS cases were validated. In a future study, more cases will be included for further validation.

Conclusions

Among clinical and imaging characteristics, central filling defects on CTPA and a significantly elevated D-dimer level may indicate APTE as the primary diagnosis. However, if CRP levels are elevated and neither D-dimer nor NT-proBNP levels show an increase, PAS should be considered. The presence of filling defects growing expansively in the main or bilateral pulmonary arteries, occupying the entire lumen, eclipsing the pulmonary wall, and showing a proximal bulging shape or distal grape-like sign is highly suggestive of PAS. Hyperintense filling defects on fat-suppressed T2WI and DWI accompanied by heterogeneous enhancement may strongly indicate PAS. Comprehensive analysis of clinical data and imaging features can aid in the accurate differential diagnosis of PAS and PTE.

Acknowledgments

Funding: This work was supported by the Medical and Health Science and Technology Innovation Project of CAMS Innovation Fund for Medical Sciences (Nos.

2022-I2M-C&T-B-109 and 2021-1-12M-049), the National High Level Hospital Clinical Research Funding & Elite Medical Professionals Project of China-Japan Friendship Hospital (Nos. 2022-NHLHCRF-LX-01 and ZRJY2021-BJ02), and the National Natural Science Foundation of China (No. 82272081).

Footnote

Reporting Checklist: The authors have completed the STROBE reporting checklist. Available at https://qims.amegroups.com/article/view/10.21037/qims-23-992/rc

Conflicts of Interest: All authors have completed the ICMJE uniform disclosure form (available at https://qims.amegroups.com/article/view/10.21037/qims-23-992/coif). The authors have no conflicts of interest to declare.

Ethical Statement: The authors are accountable for all aspects of the work in ensuring that questions related to the accuracy or integrity of any part of the work are appropriately investigated and resolved. This study was conducted in accordance with the Declaration of Helsinki (as revised in 2013) and was approved by the institutional review board of the China-Japan Friendship Hospital (No. 2023-KY-070). Informed consent was waived due to the retrospective nature of this study.

References

1. Ozbek C, Emrecan B, Calli AO, Gurbuz A. Intimal sarcoma of the pulmonary artery with retrograde extension into the pulmonic valve and right ventricle. Tex Heart Inst J 2007;34:119-21.
2. Mandelstamm M. Über primäre Neubildungen des Herzens. Virchows Arch Pathol Anat Physiol Klin Med 1923;245:43-54.
3. Gan HL, Zhang JQ, Zhou QW, Xiao W, Gao YM, Liu S, Wang PS. Surgical treatment of pulmonary artery sarcoma. J Thorac Cardiovasc Surg 2011;142:1469-72.
4. Liu MX, Ma ZH, Jiang T, Guo XJ, Yu FF, Yang YH, Zhai ZG. Differential Diagnosis of Pulmonary Artery Sarcoma and Central Chronic Pulmonary Thromboembolism Using CT and MR Images. Heart Lung Circ 2018;27:819-27.
5. Liu M, Luo C, Wang Y, Guo X, Ma Z, Yang Y, Zhang T. Multiparametric MRI in differentiating pulmonary artery sarcoma and pulmonary thromboembolism: a preliminary experience. Diagn Interv Radiol 2017;23:15-21.
6. Huo L, Moran CA, Fuller GN, Gladish G, Suster S. Pulmonary artery sarcoma: a clinicopathologic and immunohistochemical study of 12 cases. Am J Clin Pathol 2006;125:419-24.
7. Wang HP, Song W, Liu S, Gao Y, An YQ, Hou ZH, Xiong CM, Hua L, Sun Y, Lyu B. Differential diagnosis between pulmonary artery sarcoma and central chronic pulmonary thromboembolism:a preliminary study on CT signs. Zhonghua Jie He He Hu Xi Za Zhi 2022;45:269-75.
8. Kim C, Kim MY, Kang JW, Song JS, Lee KY, Kim SS. Pulmonary Artery Intimal Sarcoma versus Pulmonary Artery Thromboembolism: CT and Clinical Findings. Korean J Radiol 2018;19:792-802.
9. Gan HL, Zhang JQ, Huang XY, Yu W. The wall eclipsing sign on pulmonary artery computed tomography angiography is pathognomonic for pulmonary artery sarcoma. PLoS One 2013;8:e83200.
10. Burke AP, Virmani R. Sarcomas of the great vessels. A clinicopathologic study. Cancer 1993;71:1761-73.
11. Assi T, Kattan J, Rassy E, Moussa T, Nassereddine H, Honore C, Adam J, Terrier P, Dumont S, Mir O, Le Cesne A. A comprehensive review on the diagnosis and management of intimal sarcoma of the pulmonary artery. Crit Rev Oncol Hematol 2020;147:102889.
12. Zhang S, Zhang Y, Liu M, Tao X, Xie W, Wan J, Zhai Z. Radiological, histopathological findings, and clinical outcome of pulmonary artery sarcoma. Pulm Circ 2021;11:2045894020940537.
13. Pu X, Song M, Huang X, Zhu G, Chen D, Gan H, Huang L. Clinical and radiological features of pulmonary artery sarcoma: A report of nine cases. Clin Respir J 2018;12:1820-9.
14. Cox JE, Chiles C, Aquino SL, Savage P, Oaks T. Pulmonary artery sarcomas: a review of clinical and radiologic features. J Comput Assist Tomogr 1997;21:750-5.

15. De Luca F, Modolon C, Buia F, Attinà D, Fughelli P, Bacchi Reggiani ML, Galiè N, Zompatori M. Densitometric CT evaluation of acute and chronic thromboembolic filling defects of the pulmonary arteries before and after contrast injection. Radiol Med 2012;117:979-91.
16. Attinà D, Niro F, Tchouanté P, Mineo G, Russo V, Palazzini M, Galiè N, Fanti S, Lovato L, Zompatori M. Pulmonary artery intimal sarcoma. Problems in the differential diagnosis. Radiol Med 2013;118:1259-68.
17. Mussot S, Ghigna MR, Mercier O, Fabre D, Fadel E, Le Cesne A, Simonneau G, Dartevelle P. Retrospective institutional study of 31 patients treated for pulmonary artery sarcoma. Eur J Cardiothorac Surg 2013;43:787-93.
18. Restrepo CS, Betancourt SL, Martinez-Jimenez S, Gutierrez FR. Tumors of the pulmonary artery and veins. Semin Ultrasound CT MR 2012;33:580-90.
19. Koh DM, Collins DJ. Diffusion-weighted MRI in the body: applications and challenges in oncology. AJR Am J Roentgenol 2007;188:1622-35.
20. Palm V, Rengier F, Rajiah P, Heussel CP, Partovi S. Acute Pulmonary Embolism: Imaging Techniques, Findings, Endovascular Treatment and Differential Diagnoses. Rofo 2020;192:38-49.
21. Moore AJE, Wachsmann J, Chamarthy MR, Panjikaran L, Tanabe Y, Rajiah P. Imaging of acute pulmonary embolism: an update. Cardiovasc Diagn Ther 2018;8:225-43.
22. Ito K, Kubota K, Morooka M, Shida Y, Hasuo K, Endo H, Matsuda H. Diagnostic usefulness of 18F-FDG PET/CT in the differentiation of pulmonary artery sarcoma and pulmonary embolism. Ann Nucl Med 2009;23:671-6.
23. Ren J, Li H, Zhang Q, Liu E, Zeng B, Huang Y, Wang L, Jiang L. Clinical utility of (18)F-FDG PET/CT imaging in patients with pulmonary artery sarcoma. EJNMMI Res 2022;12:18.
24. Suto H, Suto M, Inui Y, Okamura A. Difficulty in Distinguishing Pulmonary Arterial Intimal Sarcoma from Pulmonary Thromboembolism Using FDG PET/CT. In Vivo 2022;36:1519-22.

Cite this article as: Guo R, Yang H, Xi L, Liu A, Deng M, Liu H, Gao Q, Xie W, Zhen Y, Huang Z, Liu M. Comparison of pulmonary artery sarcoma and pulmonary thromboembolism according to clinical and computed tomography pulmonary angiography and magnetic resonance imaging characteristics: a single-center retrospective study. Quant Imaging Med Surg 2024;14(2):1686-1698. doi: 10.21037/qims-23-992

Supplementary

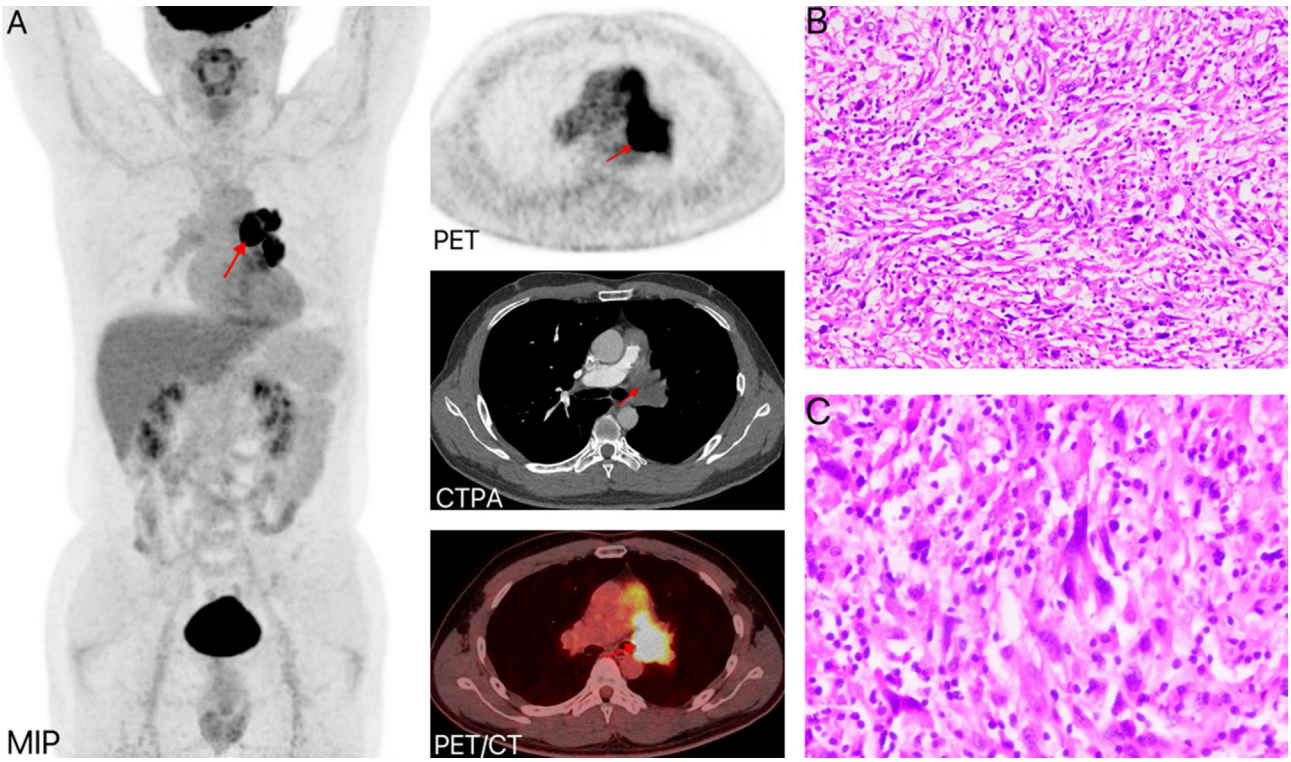

Figure S1 A 41-year-old man with a pathological diagnosis of pulmonary artery sarcoma. (A) The lesion showed intense fluorodeoxyglucose uptake (maximum standardized uptake value =12.3) on the MIP, axial PET, and fused PET-CT images, and filling defects on the CTPA (red arrows). (B,C) Histopathology indicated an abundance of malignant spindle cells with high cellularity and a high nuclear:cytoplasmic ratio (B: HE staining, ×200; C: HE staining, ×400). MIP, maximum intensity projection; PET, positron emission tomography; CTPA, computed tomography pulmonary angiography; CT, computed tomography; HE, hematoxylin and eosin.

https://dx.doi.org/10.21037/qims-23-992